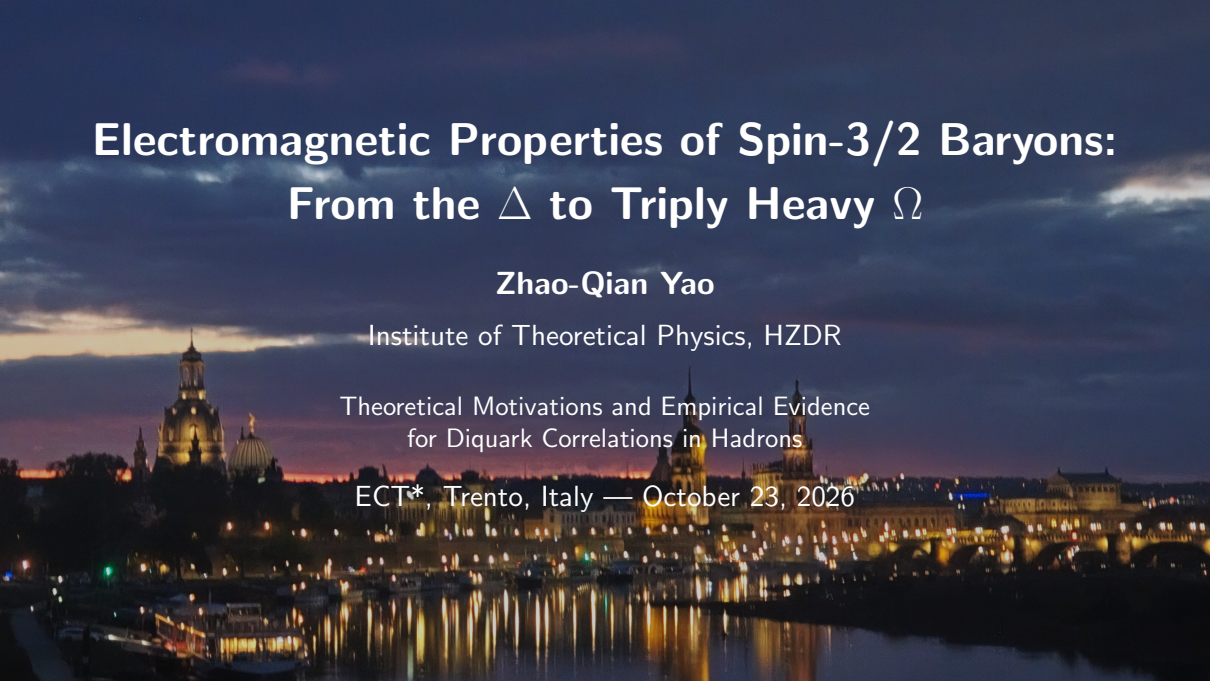
Electromagnetic Properties of Spin-3/2 Baryons: From the Δ to Triply Heavy Ω

Zhao-Qian Yao

Institute of Theoretical Physics, HZDR

Theoretical Motivations and Empirical Evidence
for Diquark Correlations in Hadrons

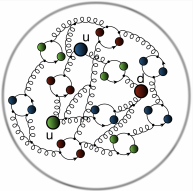
ECT*, Trento, Italy — October 23, 2026



Baryons and QCD

HZDR
HELMHOLTZ ZENTRUM
DRESDEN ROSSENDORF

Proton

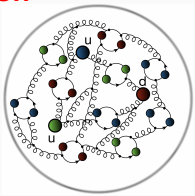


- Proton(p): $u + u + d$; Neutron(n): $d + d + u$.

Baryons and QCD

HZDR
HELMHOLTZ ZENTRUM
DRESDEN ROSSENDORF

Proton

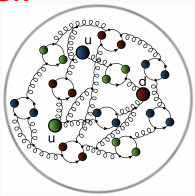


- Proton(p): $u + u + d$; Neutron(n): $d + d + u$.
- infinitely many gluons and sea-quark.

Baryons and QCD

HZDR
HELMHOLTZ ZENTRUM
DRESDEN ROSSENDORF

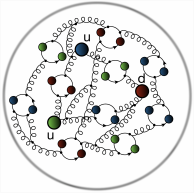
Proton

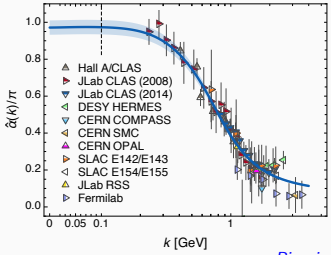


- Proton(p): $u + u + d$; Neutron(n): $d + d + u$.
- infinitely many gluons and sea-quark.
- These quarks and gluons are bound together by the strong interactions, described by quantum chromodynamics (QCD).

Baryons and QCD

Proton





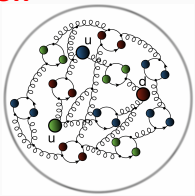
Binosi et al.

- Proton(p): $u + u + d$; Neutron(n): $d + d + u$.
- infinitely many gluons and sea-quark.
- These quarks and gluons are bound together by the strong interactions, described by quantum chromodynamics (QCD).
- QCD's Running Coupling is getting large as energy scales decrease.

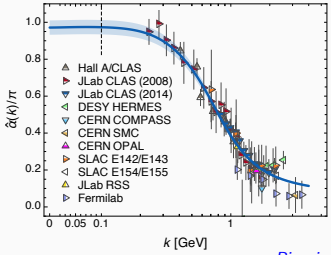
Baryons and QCD

HELMHOLTZ ZENTRUM DRESDEN ROSSENDORF

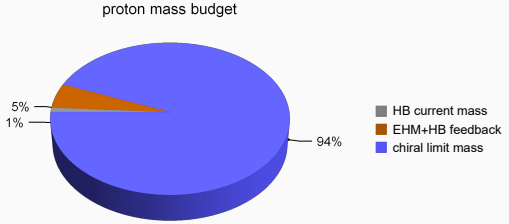
Proton



- Proton(p): $u + u + d$; Neutron(n): $d + d + u$.
- infinitely many gluons and sea-quark.
- These quarks and gluons are bound together by the strong interactions, described by quantum chromodynamics (QCD).
- QCD's Running Coupling is getting large as energy scales decrease.



Binosi et al.



Dyson-Schwinger Equations

HZDR
HELMHOLTZ ZENTRUM
DRESDEN ROSSENDORF

Dyson-Schwinger Equations (DSEs) are a system of infinitely coupled equations for Schwinger functions.

DSEs provide a widely used approach to hadron structure.

[Craig D. Roberts et al., Prog. Part. Nucl. Phys. 33 (1994) 477-575]

E-mail: z.yao@hzdr.de

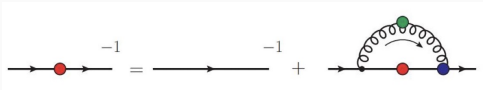
Dyson-Schwinger Equations

Dyson-Schwinger Equations (DSEs) are a system of infinitely coupled equations for Schwinger functions.

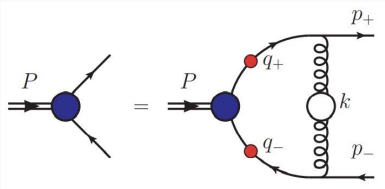
DSEs provide a widely used approach to hadron structure.

[Craig D. Roberts et al., Prog. Part. Nucl. Phys. 33 (1994) 477-575]

- Gap Equation: DSEs for quark propagator: $S(p)$

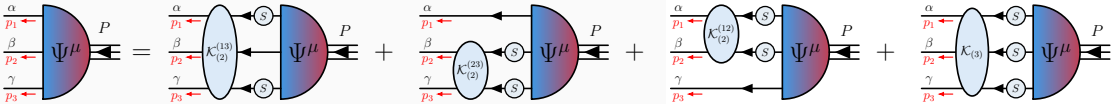


- Bethe-Salpeter Equations: DSEs for two quark bound state: $\Gamma(q, P)$



E-mail: z.yao@hzdr.de

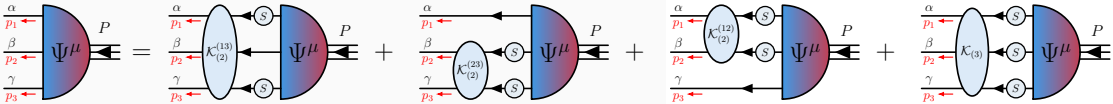
Three-body Faddeev equation



Full three-body kernel: $K_3 = K_2^{(1)} + K_2^{(2)} + K_2^{(3)} + K_3^{\mathrm{irr}}$

E-mail: z.yao@hzdr.de

Three-body Faddeev equation

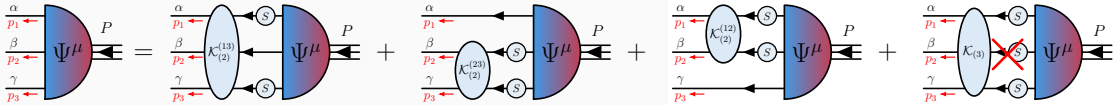


Full three-body kernel: $K_3 = K_2^{(1)} + K_2^{(2)} + K_2^{(3)} + K_3^{\text{irr}}$

- $K_2^{(1)}$: interaction of quarks $2, 3$, with quark 1 as spectator;
- $K_2^{(2)}$: interaction of quarks $1, 3$, with quark 2 as spectator;
- $K_2^{(3)}$: interaction of quarks $1, 2$, with quark 3 as spectator;
- K_3^{irr}: three-quark irreducible kernel.

The spectator is not dynamically inactive.

Three-body Faddeev equation

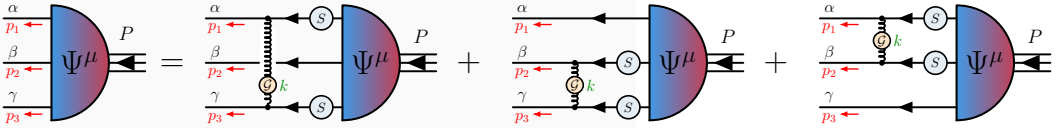


Full three-body kernel: $K_3 = K_2^{(1)} + K_2^{(2)} + K_2^{(3)} + K_3^{\text{irr}}$

- $K_2^{(1)}$: interaction of quarks $2, 3$, with quark 1 as spectator;
- $K_2^{(2)}$: interaction of quarks $1, 3$, with quark 2 as spectator;
- $K_2^{(3)}$: interaction of quarks $1, 2$, with quark 3 as spectator;
- K_3^{irr}: three-quark irreducible kernel.

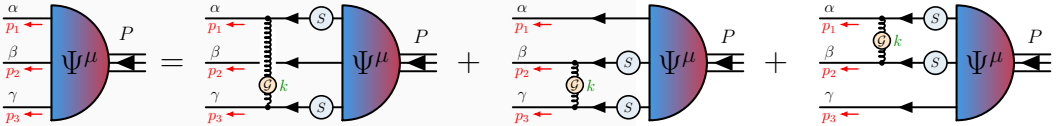
The spectator is not dynamically inactive.
The genuine three-body kernel is neglected $K_3^{\text{irr}} \approx 0$

Three-body Faddeev equation



E-mail: z.yao@hzdr.de

Three-body Faddeev equation

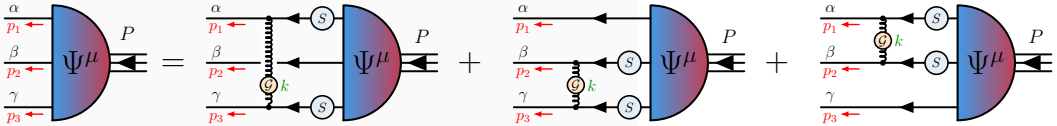


Faddeev amplitude:

$$\Psi^{\mu}_{ABCD}(p,q,P) = \psi^{\mu}_{\alpha\beta\gamma\mathcal{I}}(p,q,P) \otimes \mathrm{F}^{\mathrm{S}}_{abc} \otimes \frac{\epsilon_{rst}}{\sqrt{6}}$$

- Color structure: $\epsilon_{rst}/\sqrt{6}$; fully symmetric flavor amplitude: $\mathrm{F}^{\mathrm{S}}_{abc}$

Three-body Faddeev equation



Faddeev amplitude:

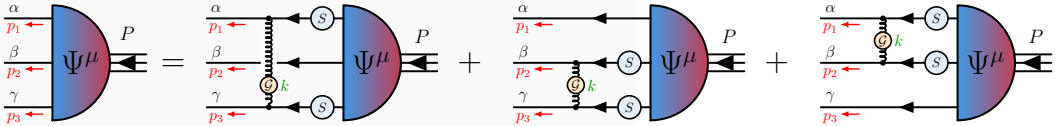
$$\Psi^{\mu}_{ABCD}(p,q,P) = \psi^{\mu}_{\alpha\beta\gamma\mathcal{I}}(p,q,P) \otimes \mathrm{F}^{\mathrm{S}}_{abc} \otimes \frac{\epsilon_{rst}}{\sqrt{6}}$$

- Color structure: $\epsilon_{rst}/\sqrt{6}$; fully symmetric flavor amplitude: $\mathrm{F}^{\mathrm{S}}_{abc}$
- Spin–momentum structure: **128 Dirac–Lorentz covariants**

$$\psi^{\mu}(p,q,P) = \sum_{l=1}^{128} f_l(p^2, q^2, z_0, z_1, z_2)\, \xi^{\mu}_l(p,q,P)$$

μ: spin-$3/2$ Lorentz index

Three-body Faddeev equation



Faddeev amplitude:

$$\Psi^{\mu}_{ABCD}(p,q,P) = \psi^{\mu}_{\alpha\beta\gamma\mathcal{I}}(p,q,P) \otimes \mathrm{F}^{\mathrm{S}}_{abc} \otimes \frac{\epsilon_{rst}}{\sqrt{6}}$$

- Color structure: $\epsilon_{rst}/\sqrt{6}$; fully symmetric flavor amplitude: $\mathrm{F}^{\mathrm{S}}_{abc}$
- Spin–momentum structure: **128 Dirac–Lorentz covariants**

$$\psi^{\mu}(p,q,P) = \sum_{l=1}^{128} f_l(p^2, q^2, z_0, z_1, z_2)\, \xi^{\mu}_l(p,q,P)$$

μ: spin-$3/2$ Lorentz index

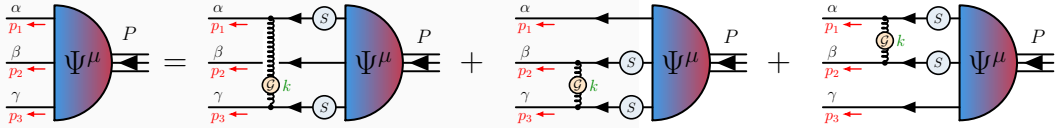
Five Lorentz-invariant variables:

$\mathfrak{T} = (p^2, q^2, z_0, z_1, z_2)$

$z_0 = \widehat{p}_T \cdot \widehat{q}_T,\ z_1 = \widehat{p} \cdot \widehat{P},\ z_2 = \widehat{q} \cdot \widehat{P}.$

T : projection transverse to P.

Three-body Faddeev equation



Faddeev amplitude:

$$\Psi^{\mu}_{ABCD}(p,q,P) = \psi^{\mu}_{\alpha\beta\gamma\mathcal{I}}(p,q,P) \otimes \mathrm{F}^{\mathrm{S}}_{abc} \otimes \frac{\epsilon_{rst}}{\sqrt{6}}$$

- Color structure: $\epsilon_{rst}/\sqrt{6}$; fully symmetric flavor amplitude: $\mathrm{F}^{\mathrm{S}}_{abc}$
- Spin–momentum structure: **128 Dirac–Lorentz covariants**

$$\psi^{\mu}(p,q,P) = \sum_{l=1}^{128} f_l(p^2,q^2,z_0,z_1,z_2)\,\xi^{\mu}_l(p,q,P)$$

μ: spin-3/2 Lorentz index

Five Lorentz-invariant variables:

$\mathfrak{T} = (p^2, q^2, z_0, z_1, z_2)$
$z_0 = \hat{p}_T \cdot \hat{q}_T,\ z_1 = \hat{p}\cdot\hat{P},\ z_2 = \hat{q}\cdot\hat{P}.$
T : projection transverse to P.

Chebyshev reconstruction:

$$f_l(\mathfrak{T}) = \sum_{n_1=0}^{N_1-1}\sum_{n_2=0}^{N_2-1}\sum_{n_0=0}^{N_0-1} T_{n_1}(z_1)T_{n_2}(z_2)T_{n_0}(z_0) \times c_l^{n_1,n_2,n_0}(p^2,q^2).$$

The spin-$3/2$ Rarita–Schwinger projector

Leading spin–momentum structure: $[S_+]^{\mu}_{\alpha\beta\gamma\mathcal{I}} = (\Lambda_+ \gamma_T^{\nu} C)_{\alpha\beta} \otimes [\mathbb{P}_+^{\mu\nu}(P)]_{\gamma\mathcal{I}}$.

E-mail: z.yao@hzdr.de

The spin-$3/2$ Rarita–Schwinger projector

HELMHOLTZ ZENTRUM DRESDEN ROSSENDORF

Leading spin–momentum structure: $[S_+]^{\mu}_{\alpha\beta\gamma\mathcal{I}} = (\Lambda_+\gamma_T^\nu C)_{\alpha\beta} \otimes [\mathbb{P}_+^{\mu\nu}(P)]_{\gamma\mathcal{I}}$.

Positive-energy, spin-$3/2$ projection

$$\mathbb{P}_+^{\mu\nu}(P) = \Lambda_+(P)(T_P^{\mu\nu} - \frac{1}{3}\gamma_T^\mu\gamma_T^\nu),\ \Lambda_+(P) = \frac{1+\gamma\cdot\widehat{P}}{2},$$

$$\widehat{P} = \frac{P}{iM}, \qquad T_P^{\mu\nu} = \delta^{\mu\nu} - \widehat{P}^\mu\widehat{P}^\nu, \qquad \gamma_T^\mu = T_P^{\mu\rho}\gamma^\rho.$$

E-mail: z.yao@hzdr.de

The spin-$3/2$ Rarita–Schwinger projector

Leading spin–momentum structure: $[S_+]^{\mu}_{\alpha\beta\gamma\mathcal{I}} = (\Lambda_+\gamma_T^\nu C)_{\alpha\beta} \otimes [\mathbb{P}_+^{\mu\nu}(P)]_{\gamma\mathcal{I}}$.

Positive-energy, spin-$3/2$ projection

$$\mathbb{P}_+^{\mu\nu}(P) = \Lambda_+(P)(T_P^{\mu\nu} - \frac{1}{3}\gamma_T^\mu\gamma_T^\nu),\ \Lambda_+(P) = \frac{1+\gamma\cdot\widehat{P}}{2},$$

$$\widehat{P} = \frac{P}{iM}, \qquad T_P^{\mu\nu} = \delta^{\mu\nu} - \widehat{P}^\mu\widehat{P}^\nu, \qquad \gamma_T^\mu = T_P^{\mu\rho}\gamma^\rho.$$

On-shell Dirac equation and constraints: $(i\gamma\cdot P + M)\mathbb{P}_+^{\mu\nu}(P) = 0$

E-mail: z.yao@hzdr.de

The spin-$3/2$ Rarita–Schwinger projector

HELMHOLTZ ZENTRUM DRESDEN ROSSENDORF

Leading spin–momentum structure: $[S_+]^{\mu}_{\alpha\beta\gamma\mathcal{I}} = (\Lambda_+\gamma_T^\nu C)_{\alpha\beta} \otimes [\mathbb{P}_+^{\mu\nu}(P)]_{\gamma\mathcal{I}}$.

Positive-energy, spin-$3/2$ projection

$$\mathbb{P}_+^{\mu\nu}(P) = \Lambda_+(P)(T_P^{\mu\nu} - \frac{1}{3}\gamma_T^\mu\gamma_T^\nu),\ \Lambda_+(P) = \frac{1+\gamma\cdot\widehat{P}}{2},$$

$$\widehat{P} = \frac{P}{iM}, \qquad T_P^{\mu\nu} = \delta^{\mu\nu} - \widehat{P}^\mu\widehat{P}^\nu, \qquad \gamma_T^\mu = T_P^{\mu\rho}\gamma^\rho.$$

On-shell Dirac equation and constraints: $(i\gamma\cdot P + M)\mathbb{P}_+^{\mu\nu}(P) = 0$

- $\mathbb{P}_+^{\mu\nu}$ represents the physical spin sum, up to normalization:

$$\mathbb{P}_+^{\mu\nu} \propto \sum_\lambda u^\mu(P,\lambda)\bar{u}^\nu(P,\lambda).$$

The spin-$3/2$ Rarita–Schwinger projector

HELMHOLTZ ZENTRUM DRESDEN ROSSENDORF

Leading spin–momentum structure: $[S_+]^{\mu}_{\alpha\beta\gamma\mathcal{I}} = (\Lambda_+\gamma_T^\nu C)_{\alpha\beta} \otimes [\mathbb{P}_+^{\mu\nu}(P)]_{\gamma\mathcal{I}}$.

Positive-energy, spin-$3/2$ projection

$$\mathbb{P}_+^{\mu\nu}(P) = \Lambda_+(P)(T_P^{\mu\nu} - \frac{1}{3}\gamma_T^\mu\gamma_T^\nu),\ \Lambda_+(P) = \frac{1+\gamma\cdot\widehat{P}}{2},$$

$$\widehat{P} = \frac{P}{iM}, \qquad T_P^{\mu\nu} = \delta^{\mu\nu} - \widehat{P}^\mu\widehat{P}^\nu, \qquad \gamma_T^\mu = T_P^{\mu\rho}\gamma^\rho.$$

On-shell Dirac equation and constraints: $(i\gamma\cdot P + M)\mathbb{P}_+^{\mu\nu}(P) = 0$

- $\mathbb{P}_+^{\mu\nu}$ represents the physical spin sum, up to normalization:

$$\mathbb{P}_+^{\mu\nu} \ \propto \ \sum_\lambda u^\mu(P,\lambda)\bar{u}^\nu(P,\lambda).$$

- All four physical spin states are encoded in one matrix.

$$\psi^\mu_{\alpha\beta\gamma\mathcal{I}}(p,q,P) \ \propto \ \sum_\lambda \Psi_{\alpha\beta\gamma}(p,q,P;\lambda)\,\bar{u}^\mu_{\mathcal{I}}(P,\lambda).$$

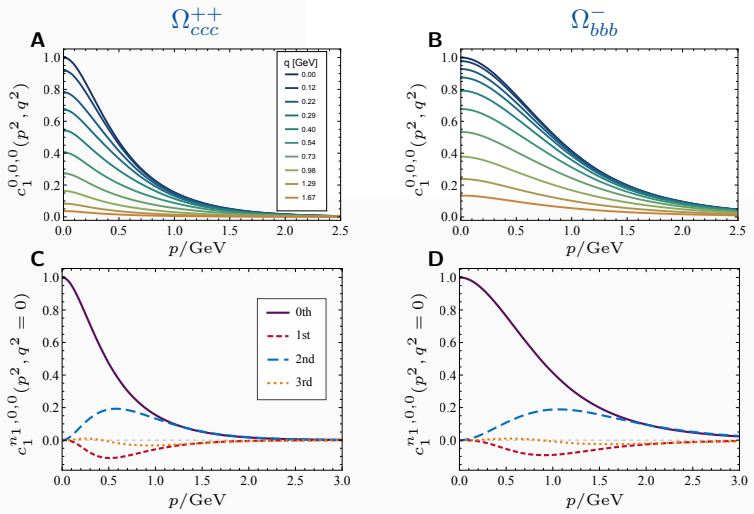
Heavy-sector Faddeev amplitudes

Calculated masses

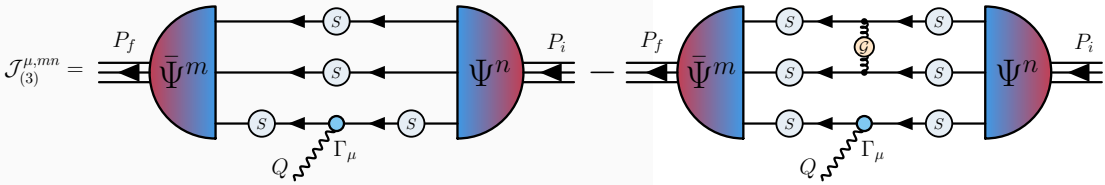
Hadron	Calc.	Expt./IQCD
η_c	2.98	2.98
J/ψ	3.12	3.10
η_b	9.40	9.40
Υ	9.50	9.46
Ω_{ccc}^{++}	4.76	4.793(9)
		4.769(6)
Ω_{bbb}^{-}	14.35	14.371(12)

All masses in GeV.

Meson and baryon masses are calculated results of the Bethe–Salpeter and Faddeev equations.



The electromagnetic current



- Gauge the three-body scattering equation.
- Use the dressed quark–photon vertex from the inhomogeneous BSE.
- Preserve the vector Ward–Takahashi identity.

$$Q_\mu \Gamma^\mu = S^{-1}(p_+) - S^{-1}(p_-)$$

Charge normalization checks the current construction.

Four spin-$3/2$ electromagnetic multipoles

HELMHOLTZ ZENTRUM DRESDEN ROSSENDORF

Spin $J = 3/2$: $2J + 1 = 4$ independent elastic electromagnetic form factors.

$$\mathcal{J}^{\mu,mn} = \mathbb{P}^{mm'}(P_f)\left\{ \left([F_1 + F_2] i\gamma^\mu - F_2 \frac{P^\mu}{M} \right) \delta^{m'n'} + \left([F_3 + F_4] i\gamma^\mu - F_4 \frac{P^\mu}{M} \right) \frac{Q^{m'} Q^{n'}}{4M^2} \right\} \mathbb{P}^{n'n}(P_i).$$

$P = (P_f + P_i)/2$, $Q = P_f - P_i$; $\mathbb{P}$: spin-3/2 projector; $\tau = Q^2/(4M^2)$.

Parity (same-parity states):
E_L: even L; M_L: odd L.
With $L \leq 2J = 3$: $E0,\ M1,\ E2,\ M3$.

Multipole form factors

G_{E0}: electric-monopole;

G_{M1}: magnetic-dipole;

G_{E2}: electric-quadrupole;

G_{M3}: magnetic-octupole.

$$G_{E0} = \left(1 + \frac{2\tau}{3}\right)(F_1 - \tau F_2) - \frac{\tau}{3}(1+\tau)(F_3 - \tau F_4),$$

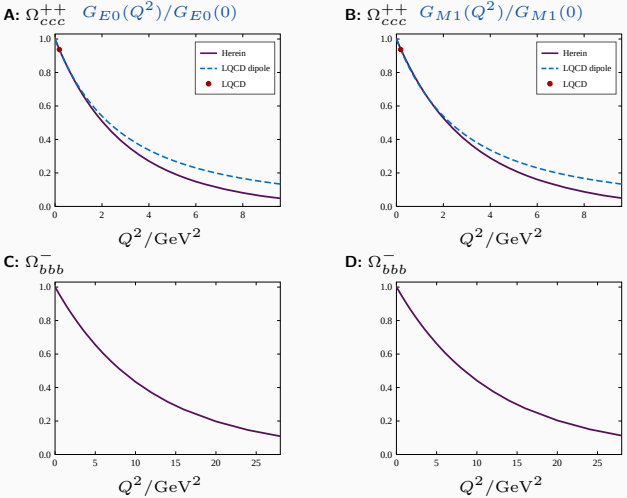
$$G_{M1} = \left(1 + \frac{4\tau}{5}\right)(F_1 + F_2) - \frac{2\tau}{5}(1+\tau)(F_3 + F_4),$$

$$G_{E2} = (F_1 - \tau F_2) - \frac{1}{2}(1+\tau)(F_3 - \tau F_4),$$

$$G_{M3} = (F_1 + F_2) - \frac{1}{2}(1+\tau)(F_3 + F_4).$$

E-mail: z.yao@hzdr.de

Electric and magnetic form factors



$G_{E0}^{\Omega_{ccc}^{++}}(0) = +2, \quad G_{E0}^{\Omega_{bbb}^{-}}(0) = -1$

Charges in units of e.

Magnetic moments: $\mu_B = \dfrac{e}{2M_B} G_{M1}(0)$

μ_B/μ_N	Ω_{ccc}^{++}	Ω_{bbb}^{-}
Here	**1.26**	$\mathbf{-0.207}$
NR Faddeev (AL1)	1.023	-0.180
hCQM	1.176(19)	$-0.194(1)$
EMS	1.10	—
SCS	1.16	—
Bag model	1.138	-0.194
lQCD	0.676(5)	—

lQCD: K. U. Can et al., Phys. Rev. D **92**, 114515 (2015).

E-mail: z.yao@hzdr.de

Radii and the heavy-quark magnetic reference

HZDR
HELMHOLTZ ZENTRUM
DRESDEN ROSSENDORF

Electric and magnetic radii

	r_{E0} [fm]	r_{M1} [fm]	r_{E0}/r_{M1}
Ω_{ccc}^{++}	0.287(1)	0.279(1)	1.029
lQCD (Ω_{ccc}^{++})	0.290(5)	0.290(5)	1.000
Ω_{bbb}^{-}	0.140(2)	0.138(3)	1.014

Ratios are calculated from the central values.

$$\frac{r_{E0}}{r_{M1}} \longrightarrow 1 \quad \text{in the heavy-quark limit.}$$

The electric-to-magnetic radius ratio moves closer to unity from charm to bottom.

Magnetic moments and heavy-quark reference

$$\mu_{\Omega_{ccc}^{++}} = 1.26\,\mu_N, \qquad \mu_{\Omega_{bbb}^{-}} = -0.207\,\mu_N$$

$$\mu_{QQQ}^{\mathrm{NR}} = 3\frac{ee_Q}{2m_Q}, \qquad G_{M1}^{\mathrm{NR}}(0) = 3e_Q\frac{M}{m_Q}$$

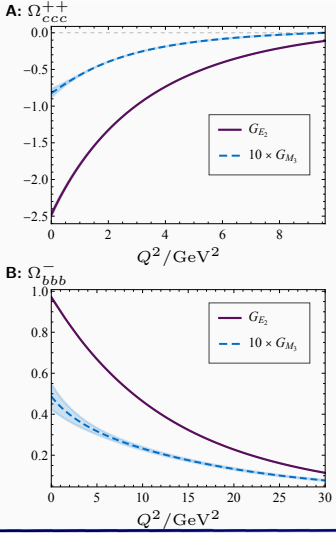
$$M \to 3m_Q: \qquad G_{M1}(0) \to 9e_Q$$

	Here	Heavy-quark limit	Deviation
Ω_{ccc}^{++}	6.40	6	6.7%
Ω_{bbb}^{-}	-3.14	-3	4.7%

The bottom result is closer to the leading heavy-quark limit.

E-mail: z.yao@hzdr.de

Higher multipoles and charge-normalized moments



Static higher moments

	Ω^{++}_{ccc}	Ω^{-}_{bbb}
$G_{E2}(0)$	$-2.48(4)$	$0.971(8)$
$G_{M3}(0)$	$-0.0825(60)$	$0.0487(64)$
$G_{E2}(0)/Q_B$	$-1.24(2)$	$-0.971(8)$
$G_{M3}(0)/Q_B$	$-0.0413(30)$	$-0.0487(64)$

$$Q_{\Omega^{++}_{ccc}} = +2, \qquad Q_{\Omega^{-}_{bbb}} = -1.$$

- The charge-normalized quadrupole magnitude decreases from charm to bottom.
- The charge-normalized octupoles are compatible within uncertainties.

E-mail: z.yao@hzdr.de

Light- and strange-sector

Meson and baryon observables

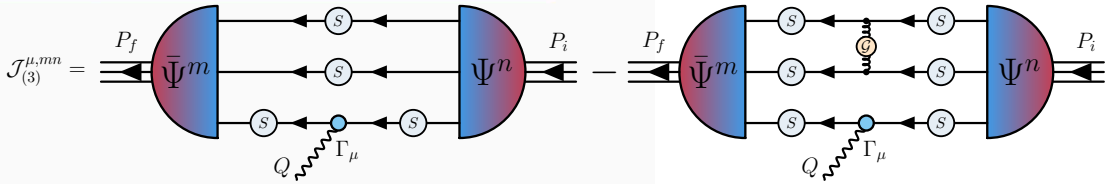
Representative results with the light/strange-sector interaction, compared with experiment. All quantities below are in GeV.

	f_π	f_K	m_{K^*}	f_{K^*}	m_ϕ	f_ϕ	m_N	m_Δ	m_Ω
Herein	0.094	0.11	0.95	0.18	1.09	0.19	0.94	1.20	1.67
Expt.	0.092	0.11	0.89	0.16	1.02	0.17	0.94	1.23	1.67

The pion and kaon masses, $m_\pi = 0.14\,\mathrm{GeV}$ and $m_K = 0.50\,\mathrm{GeV}$, fix the light- and strange-quark current masses, respectively.

E-mail: z.yao@hzdr.de

A phenomenological AMM



- Dynamical chiral symmetry breaking (DCSB) generates anomalous chromomagnetic structures in the dressed quark–gluon vertex, inducing a sizeable dressed-quark AMM beyond RL.
- We estimate the missing electromagnetic vertex dressing with a phenomenological Pauli term.

Chang, Liu and Roberts, Phys. Rev. Lett. 106, 072001 (2011).

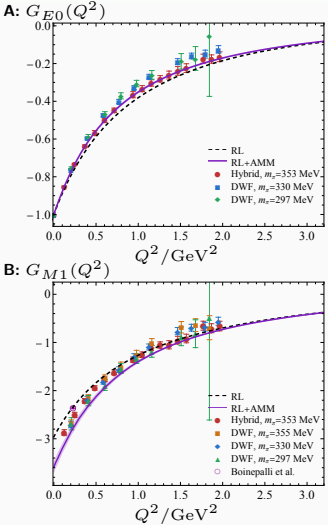
$$\Gamma^\mu = \Gamma^\mu_{\rm RL} + \Gamma^\mu_{\rm AMM},$$
$$\Gamma^\mu_{\rm AMM} = \frac{\eta}{2M^E}\sigma^{\mu\nu}Q_\nu e^{-Q^2/[4(M^E)^2]}.$$
$$M^E_u = 0.41\,{\rm GeV}, \qquad M^E_s = 0.567\,{\rm GeV},$$
$$\eta = 0.264(44), \qquad M^E_f = M_f\left((M^E_f)^2\right).$$

- The transverse term preserves the vector WTI;
- Preserves the charge conservation.

E-mail: z.yao@hzdr.de

Ω^- leading spacelike multipoles

HELMHOLTZ ZENTRUM DRESDEN ROSSENDORF



Static moments and radii

Calculation	$G_{M1}(0)$	r_{E0} [fm]	r_{M1} [fm]
RL	-2.98	0.533(02)	0.510(02)
RL+AMM	$-3.60(09)^*$	0.561(07)	0.516(05)
lQCD, 297 MeV	$-3.26(17)$	0.596(12)	0.535(29)
lQCD, extrap.	$-3.33(71)$	0.590(44)	0.567(14)

*Magnetic-moment input; not an independent prediction.

Ω^- : $r_{E0} > r_{M1}$ **in both RL and RL+AMM.**

The same ordering is found in our proton calculation:
$r_E^p \simeq 0.888\,\mathrm{fm} > r_M^p \simeq 0.820\,\mathrm{fm}.$

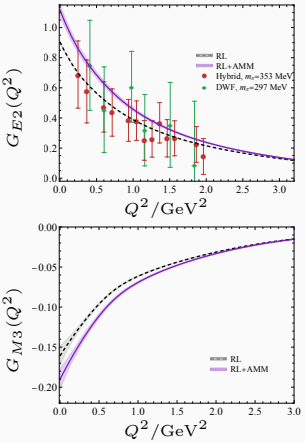
Z.-Q. Yao et al., Fundam. Res. **6**, 1409–1416 (2026).

E-mail: z.yao@hzdr.de

Ω^- higher multipoles and static moments

HELMHOLTZ ZENTRUM DRESDEN ROSSENDORF

Spacelike form factors



Static higher moments

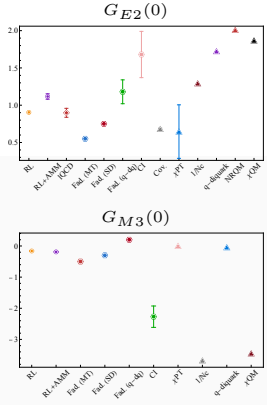
	$G_{E2}(0)$	$G_{M3}(0)$
RL	0.904(10)	$-0.161(12)$
RL+AMM	1.117(37)	$-0.190(13)$

$$\mathcal{Q} = \frac{e}{M_\Omega^2} G_{E2}(0)$$

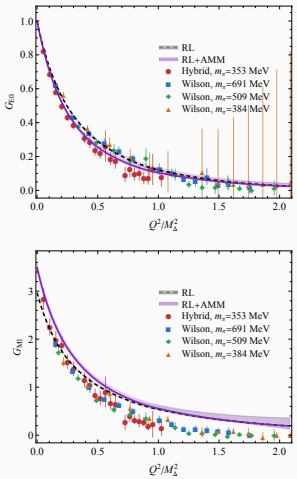
$$\mathcal{O} = \frac{e}{2M_\Omega^3} G_{M3}(0)$$

- The AMM increases both higher-moment magnitudes.
- Higher moments show substantial dependence on the dynamical framework.

Comparison with other methods



Δ: leading spacelike multipoles



Magnetic dipole and electromagnetic radii

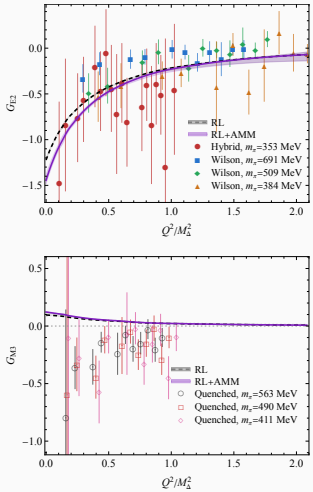
Calculation	$G_{M1}(0)$	r_{E0} [fm]	r_{M1} [fm]
RL	2.967	0.751(5)	0.716(4)
RL+AMM	3.49(9)	0.784(8)	0.720(4)
Expt.	$3.55^{+4.60}_{-4.72}$	—	—
lQCD, Hybrid 353	3.04(24)	0.635(21)	0.500(33)
lQCD, Wilson 691	2.589(78)	0.529(17)	0.424(13)
lQCD, Wilson 509	2.68(13)	0.595(11)	0.489(19)
lQCD, Wilson 384	2.35(16)	0.639(15)	0.480(18)

$G_{M1}^{\Omega^-}(0) = -3.60(9)$. $\tau_\Delta \simeq 5.6 \times 10^{-24}\,\mathrm{s}$ (strong decay),
$\tau_{\Omega^-} = 8.21(11) \times 10^{-11}\,\mathrm{s}$ (weak decay).

The AMM enhances $G_{M1}(0)$ and r_{E0}; $r_{E0} > r_{M1}$ in both calculations.

E-mail: z.yao@hzdr.de

Δ: higher multipoles and static moments



Static higher moments

	$G_{E2}(0)$	$G_{M3}(0)$
RL	$-1.222(4)$	$0.10(1)$
RL+AMM	$-1.443(38)$	$0.13(1)$

$G_{E0}(0) = +1$: Δ^+ convention.

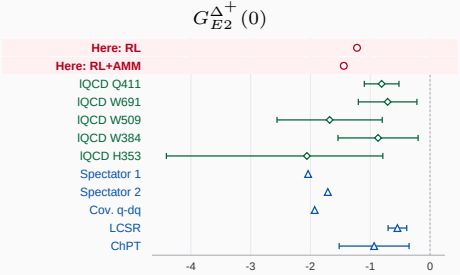
$$\mathcal{Q} = \frac{e}{M_\Delta^2} G_{E2}(0),$$

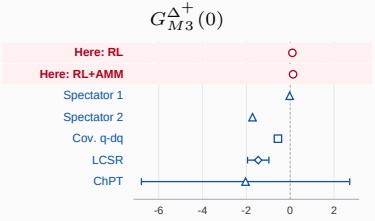
$$\mathcal{O} = \frac{e}{2M_\Delta^3} G_{M3}(0).$$

The AMM enhances both higher-moment magnitudes.

E-mail: z.yao@hzdr.de

Δ: static higher moments in comparison





Static higher moments

	$G_{E2}(0)$	$G_{M3}(0)$
RL	$-1.222(4)$	$0.10(1)$
RL+AMM	$-1.443(38)$	$0.13(1)$

$G_{E0}(0) = +1$: Δ^+ convention.

$$\mathcal{Q} = \frac{e}{M_\Delta^2} G_{E2}(0),$$

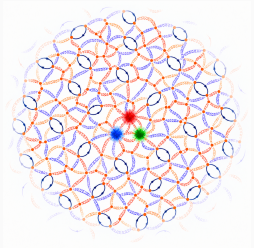
$$\mathcal{O} = \frac{e}{2M_\Delta^3} G_{M3}(0).$$

The AMM enhances both higher-moment magnitudes.

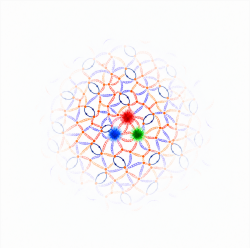
E-mail: z.yao@hzdr.de

Electric and magnetic radii across flavors

Baryon	r_{E0} [fm]	r_{M1} [fm]	$\frac{r_{E0}}{r_{M1}} - 1$
Δ	0.784(8)	0.720(4)	0.089(13)
Ω^-	0.561(07)	0.516(05)	0.087(17)
Ω^{++}_{ccc}	0.287(1)	0.279(1)	0.029(5)
Ω^-_{bbb}	0.140(2)	0.138(3)	0.014(26)



More extended dressing



More compact distribution

1. **Smaller radii, harder form factors.**
   Long-range dressing becomes relatively less important as the quarks become heavier: baryons become more compact and their form factors harder.

$$S(p) = \frac{Z(p^2)}{i\gamma\cdot p + M(p^2)} = Z(p^2)\frac{-i\gamma\cdot p + M(p^2)}{p^2 + M^2(p^2)}$$

   $Z = 1/A$, $M = B/A$; Euclidean conventions.

2. **Electric and magnetic radii converge.**
   In the simplest nonrelativistic heavy-quark limit, charge and magnetization share the same spatial profile, giving $r_{E0}/r_{M1} = 1$. Their difference therefore probes nontrivial quark–gluon dynamics beyond this limit.

E-mail: z.yao@hzdr.de

Summary and outlook

- The bottom system is more compact than the charm system.
- Heavy-sector magnetic and radius diagnostics move toward leading NR behavior.
- For Ω^-, a fitted AMM term modifies magnetic and higher multipoles.
- The timelike matching estimate needs stronger numerical and dynamical control.
- The Δ extends the comparison to light quarks; improve the current beyond the present vertex Ansatz.

Thank you!

E-mail: z.yao@hzdr.de

Backup: current projections

$$\mathcal{T}_1^{\mu,mn} = \widehat{P}^\mu \widehat{P}^m \widehat{P}^n, \qquad \mathcal{T}_2^{\mu,mn} = \widehat{P}^\mu \delta^{mn},$$
$$\mathcal{T}_3^{\mu,mn} = \gamma^\mu \widehat{P}^m \widehat{P}^n, \qquad \mathcal{T}_4^{\mu,mn} = \gamma^\mu \delta^{mn}.$$
$$g_i(Q^2) = \mathrm{Tr}_D[\mathcal{T}_i^{\mu,mn} \mathcal{J}^{\mu,mn}], \qquad i = 1, \ldots, 4.$$

- Write the on-shell current as $\mathcal{J} = \sum_{j=1}^{4} F_j \mathcal{K}_j$, including the spin-$3/2$ projectors in $\mathcal{K}_j$.
- Contract and trace: $g_i = \sum_j A_{ij} F_j$, with $A_{ij} = \mathrm{Tr}_D[\mathcal{T}_i \mathcal{K}_j]$.
- At nonzero Q^2, invert this system and convert F_j to $G_{E0}, G_{M1}, G_{E2}, G_{M3}$.

Backup: four form factors from scalar projections

HELMHOLTZ ZENTRUM DRESDEN ROSSENDORF

$$\tau = \frac{Q^2}{4M^2}, \qquad g_i = g_i(Q^2)$$

$$G_{E0} = \frac{i(2g_1 - g_2)}{4\sqrt{1+\tau}},$$

$$G_{M1} = \frac{9iM^2}{10Q^2}\left[\frac{2g_1 - g_2}{\sqrt{1+\tau}} - 2g_3 + g_4\right],$$

$$G_{E2} = -\frac{3iM^2}{2Q^4\sqrt{1+\tau}}\left[-g_2Q^2 + 2g_1(6M^2 + Q^2)\right],$$

$$G_{M3} = \frac{3iM^4}{Q^6\sqrt{1+\tau}}\Big[g_2Q^2 - 2g_1(5M^2 + Q^2) + \left(-g_4Q^2 + 2g_3(5M^2 + Q^2)\right)\sqrt{1+\tau}\Big].$$

The apparent inverse powers of Q^2 cancel analytically, but amplify numerical errors.

Backup: why extrapolate G_{M3} to $Q^2 = 0$?

HELMHOLTZ ZENTRUM DRESDEN ROSSENDORF

$$x = Q^2, \qquad G_{M3}(x) = \frac{3iM^4}{x^3\sqrt{1 + x/(4M^2)}}\,\mathcal{N}_3(x).$$

- A finite static value requires $\mathcal{N}_3(x) = \mathcal{O}(x^3)$: lower-order terms cancel between the scalar projections.
- Numerical integration and subtraction errors spoil this delicate cancellation at very small x.

$$\delta G_{M3}(x) = \frac{3iM^4\,\delta\mathcal{N}_3(x)}{x^3\sqrt{1 + x/(4M^2)}}.$$

- Reconstruct the form factor from numerically stable, nonzero-Q^2 points with SPM; take the limit to obtain $G_{M3}(0)$.
- The spread of accepted reconstructions estimates reconstruction sensitivity, not the full truncation uncertainty.

The difficulty is numerical cancellation, not a divergence of the magnetic octupole moment.

E-mail: z.yao@hzdr.de

Backup: Qin–Chang interaction

$$\mathcal{G}(s) = \frac{8\pi^2 D}{\omega^4} e^{-s/\omega^2} + \frac{8\pi^2 \gamma_m \mathcal{F}(s)}{\ln\left[\tau + (1 + s/\Lambda_{\mathrm{QCD}}^2)^2\right]}$$

$$\mathcal{F}(s) = \frac{1 - e^{-s/(4m_t^2)}}{s}, \qquad s = k^2, \qquad \tau = e^2 - 1$$

- Infrared strength and range are controlled by D and ω.
- The ultraviolet term implements the one-loop running behavior.
- Within each sector, the interaction is used consistently in the gap, Bethe–Salpeter and Faddeev equations.

Qin–Chang interaction: Qin et al., Phys. Rev. C 84, 042202(R) (2011).

Backup: light- and heavy-sector parameters

HELMHOLTZ ZENTRUM DRESDEN ROSSENDORF

Parameter	Light system	Heavy system
ω [GeV]	0.5	0.8
D [GeV^2]	1.024	0.27
ωD [GeV^3]	$0.8^3 = 0.512$	0.216

The light/strange and heavy sectors use different interaction calibrations.

E-mail: z.yao@hzdr.de

Backup: benchmark and source scope

HELMHOLTZ ZENTRUM DRESDEN ROSSENDORF

[GeV]	m_N	m_Δ	m_Ω
Strange-sector calculation	0.94	1.20	1.67
Experiment	0.94	1.23	1.67

- All numerical results and scientific plots come from the two supplied drafts.
- Lattice and experimental comparisons retain their manuscript citations.
- Reference artwork and typography follow the Nstar report.

E-mail: z.yao@hzdr.de

Backup: effective timelike form factor

HELMHOLTZ ZENTRUM DRESDEN ROSSENDORF

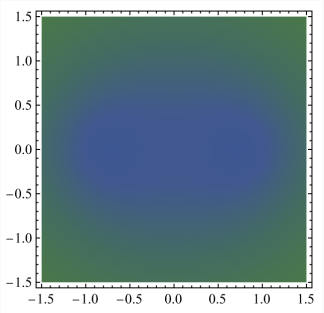
$$\tau = q^2/(4M_\Omega^2)$$

$$|G_{\rm eff}|^2 = \frac{1}{1+1/(2\tau)}\left\{\frac{10}{9}|G_{M1}|^2 + \frac{16}{15}\tau^2|G_{M3}|^2 + \frac{1}{2\tau}\left(2|G_{E0}|^2 + \frac{8}{9}\tau^2|G_{E2}|^2\right)\right\}$$

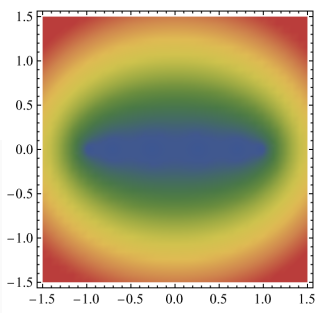
E-mail: z.yao@hzdr.de

Backup: angular analytic continuation

$n = 2$



$n = 6$



- Moving-frame angular variables can become complex.
- Higher Chebyshev moments amplify small numerical errors.

E-mail: z.yao@hzdr.de